

Land cover regulates the spatial variability of temperature response to the direct radiative effect of aerosols

T. Chakraborty^{1*}, X. Lee¹

1. School of Forestry and Environmental Studies, Yale University, New Haven, Connecticut, USA

Contents of this file

Figures S1 to S11

Table S1

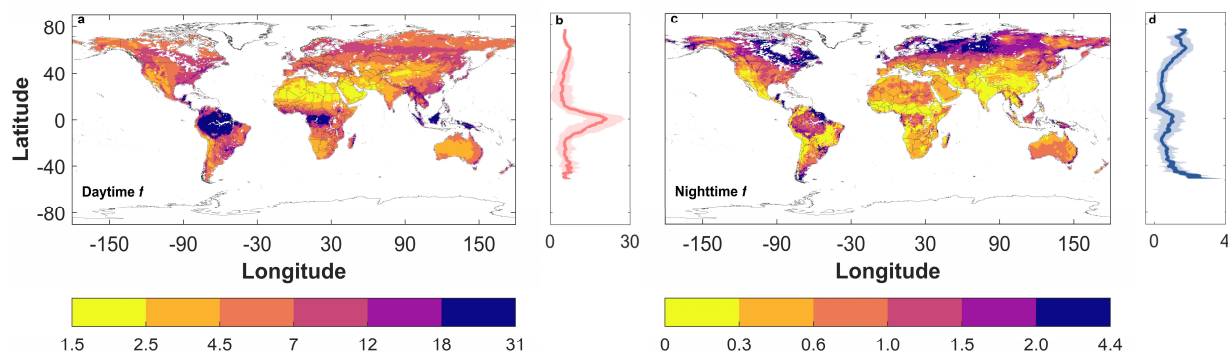


Figure S1. Global spatial patterns of daytime (a) and nighttime (c) f (unitless) for 2008-2017. Non-linear color maps are used to better visualize the spatial variations throughout the world. The corresponding zonal characteristics are given in panels b (daytime f) and d (nighttime f). The solid lines represent the zonal means, while the shaded regions show standard deviations at each degree of latitude.

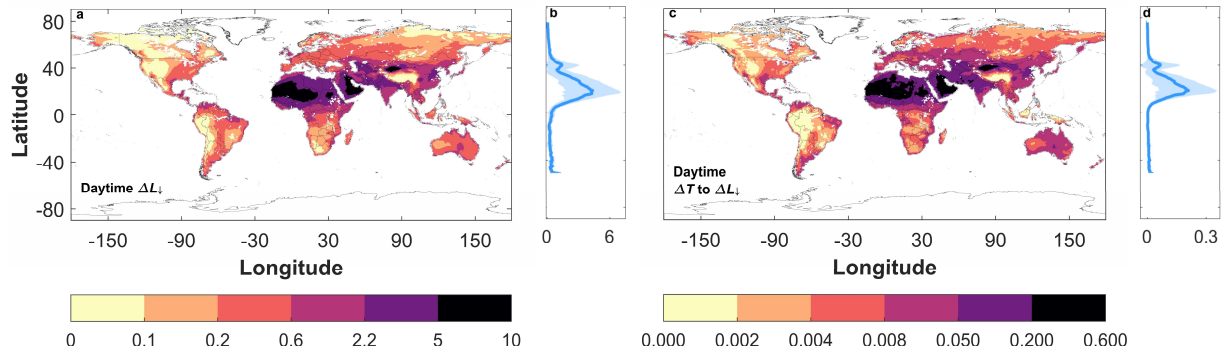


Figure S2. a, Global spatial patterns of daytime surface longwave RE (ΔL_{\downarrow} ; in W m^{-2}) and **c**, global spatial patterns of daytime temperature perturbation ΔT to daytime longwave RE (in K) for 2008-2017. Non-linear color maps are used to better visualize the spatial variations throughout the world. The corresponding zonal characteristics are given in panels **b** (daytime ΔL_{\downarrow}) and **d** (temperature perturbation to daytime ΔL_{\downarrow}). The solid lines represent the zonal means, while the shaded regions show standard deviations at each degree of latitude.

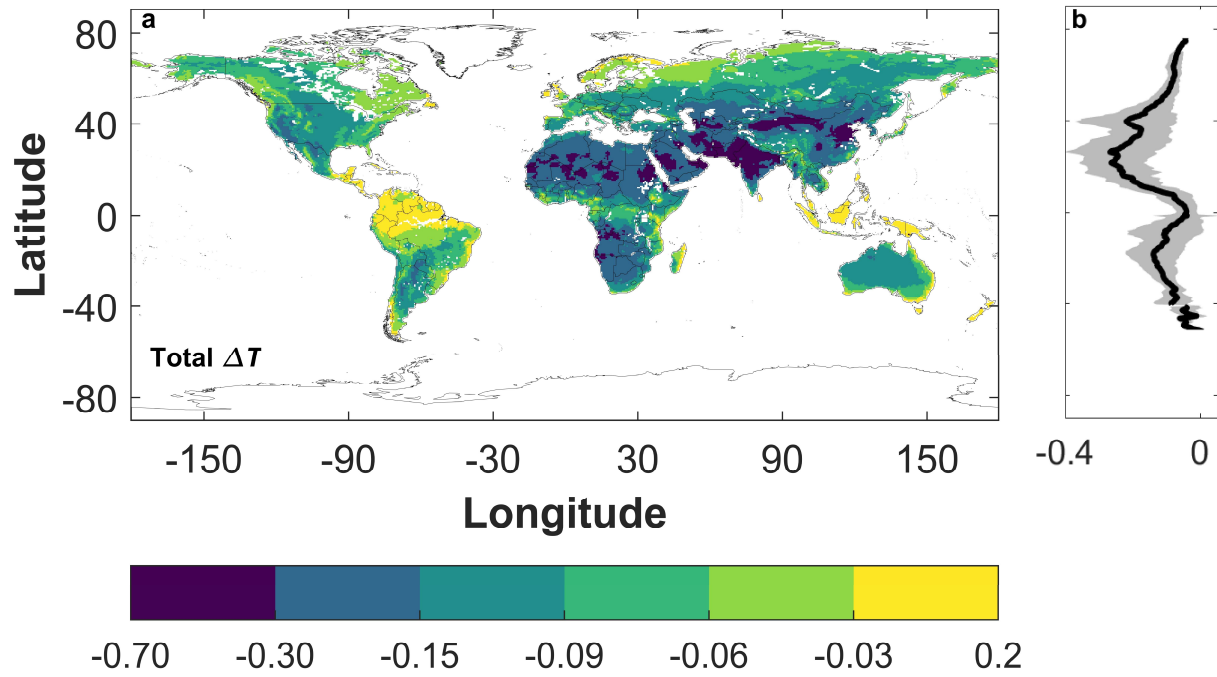


Figure S3. a, Global spatial patterns of 24-hour ΔT (in K) and **b**, the zonal characteristics of 24-hour ΔT for 2008-2017. Non-linear color maps are used to better visualize the spatial variations throughout the world. The solid line in panel **b** represents the zonal mean, while the shaded regions show standard deviations at each degree of latitude.

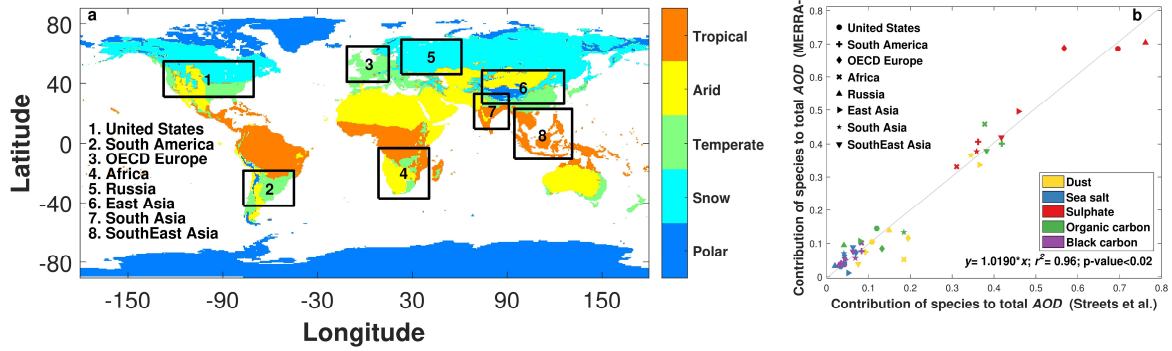


Figure S4. a, Distribution of Koppen-Geiger climate zones and regions of interest used in this study and **b**, comparison of contribution of different species to total AOD for MERRA-2 and *Street et al.* [2009].

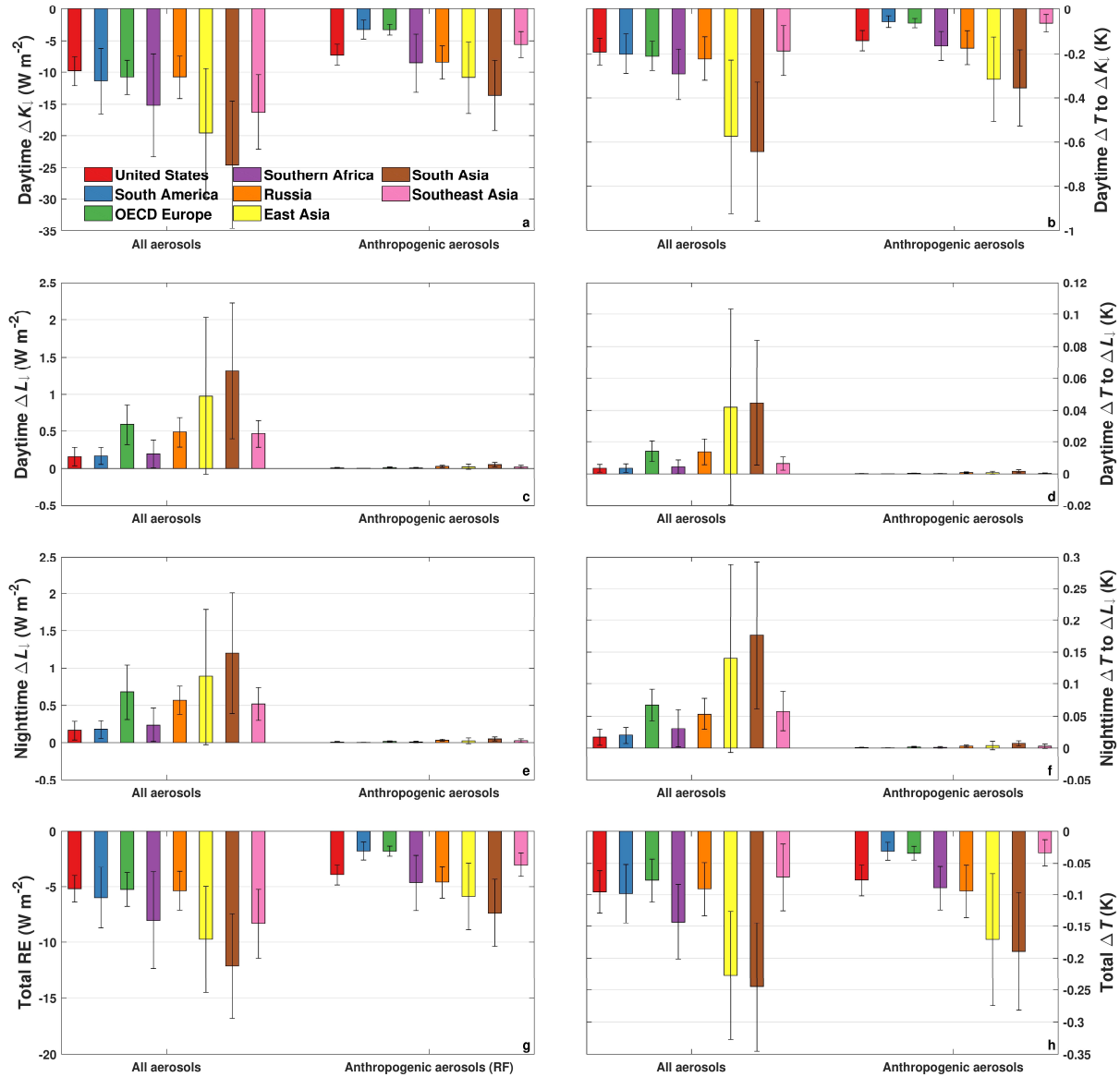


Figure S5. Contribution of anthropogenic aerosols to **a**, daytime shortwave RE (ΔK_{\downarrow}), **b**, daytime temperature perturbation due to shortwave RE, **c**, daytime longwave RE (ΔL_{\downarrow}), **d**, daytime temperature perturbation due to longwave RE, **e**, nighttime longwave RE (ΔL_{\downarrow}), **f**, nighttime temperature perturbation; **g**, total RE at the surface, and **h**, 24-hour mean temperature perturbation for 1980-2006.

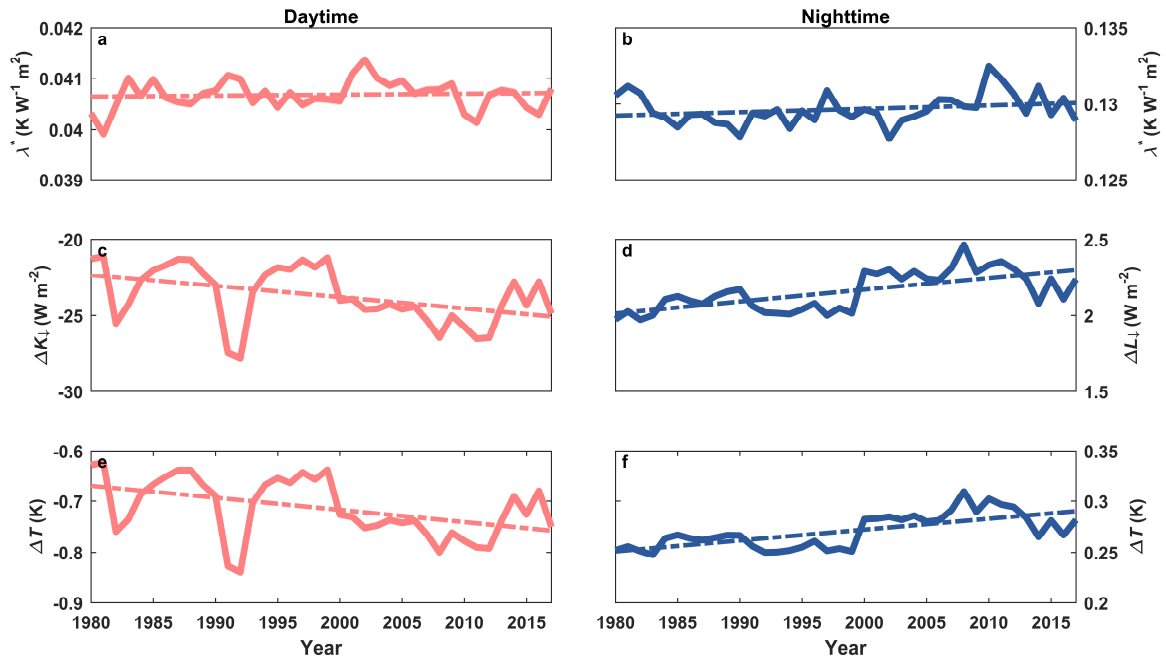


Figure S6. Long-term trends in **a**, daytime apparent surface climate sensitivity (λ^*), **b**, nighttime λ^* , **c**, daytime surface shortwave RE (ΔK_{\downarrow}), **d**, nighttime surface longwave RE (ΔL_{\downarrow}), **e**, daytime temperature perturbation, and **f**, nighttime temperature perturbation for the arid climate zone. The dashed lines show the linear trends of the temporal variation. All long-term trends are statistically significant (p -value < 0.01).

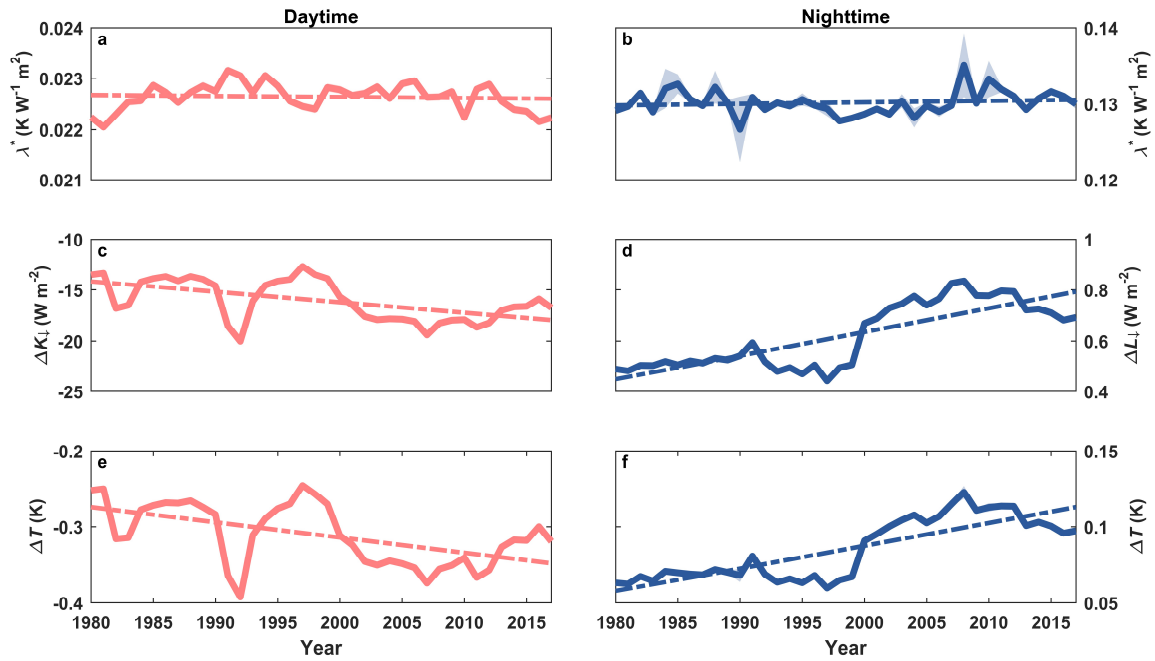


Figure S7. Long-term trends in **a**, daytime apparent surface climate sensitivity (λ^*), **b**, nighttime λ^* , **c**, daytime surface shortwave RE (ΔK_{\downarrow}), **d**, nighttime surface longwave RE (ΔL_{\downarrow}), **e**, daytime temperature perturbation, and **f**, nighttime temperature perturbation in the temperate climate zone. The dashed lines show the linear trends of the temporal variation. All long-term trends are statistically significant (p -value < 0.01).

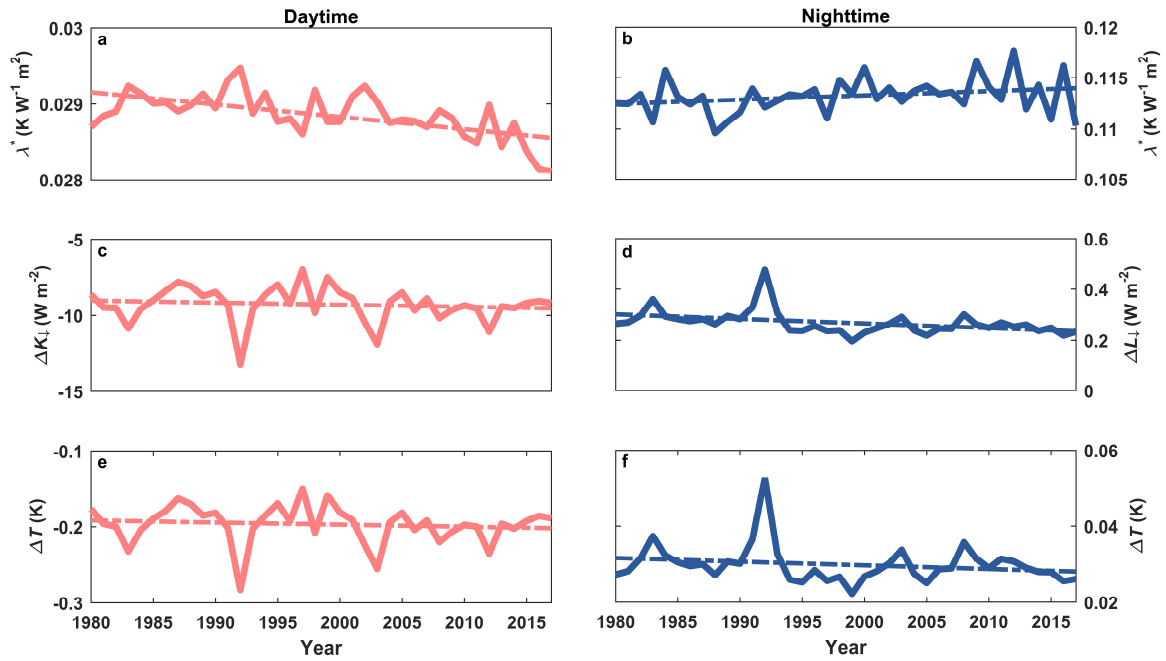


Figure S8. Long-term trends in **a**, daytime apparent surface climate sensitivity (λ^*), **b**, nighttime λ^* , **c**, daytime surface shortwave RE (ΔK_{\downarrow}), **d**, nighttime surface longwave RE (ΔL_{\downarrow}), **e**, daytime temperature perturbation, and **f**, nighttime temperature perturbation in the snow climate zone. The dashed lines show the linear trends of the temporal variation. All long-term trends, except for nighttime ΔL_{\downarrow} , are statistically significant (p -value < 0.01).

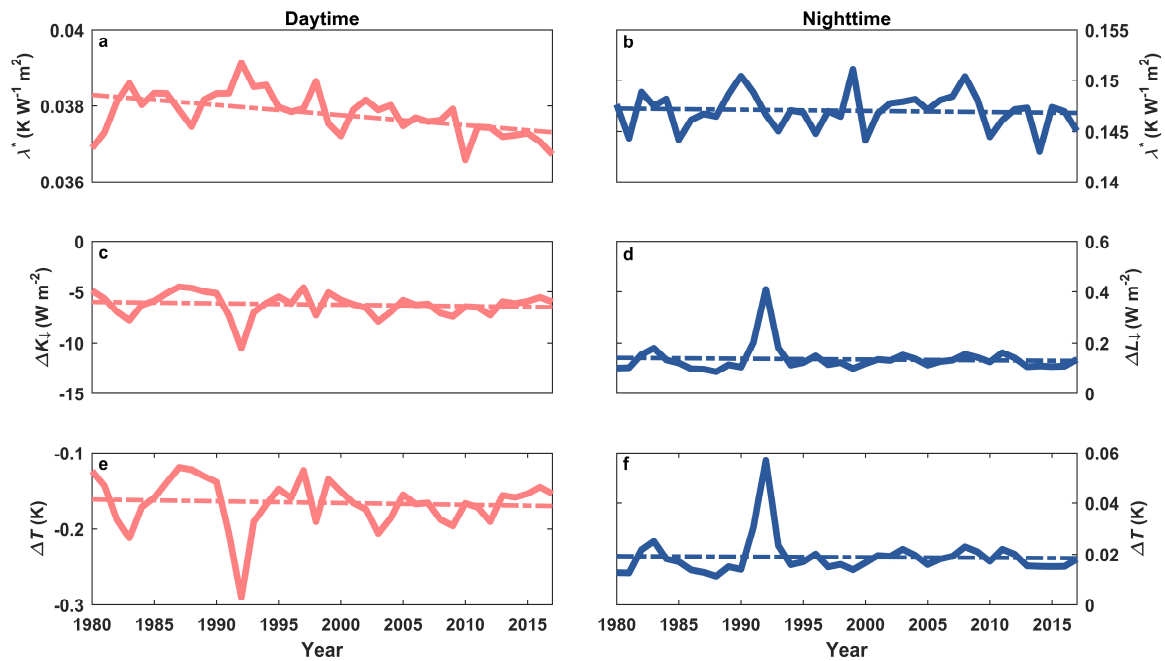


Figure S9. Long-term trends in **a**, daytime apparent surface climate sensitivity (λ^*), **b**, nighttime λ^* , **c**, daytime surface shortwave RE (ΔK_{\downarrow}), **d**, nighttime surface longwave RE (ΔL_{\downarrow}), **e**, daytime temperature perturbation, and **f**, nighttime temperature perturbation in the polar climate zone. The dashed lines show the linear trends of the temporal variation. All long-term trends are statistically significant (p -value < 0.01).

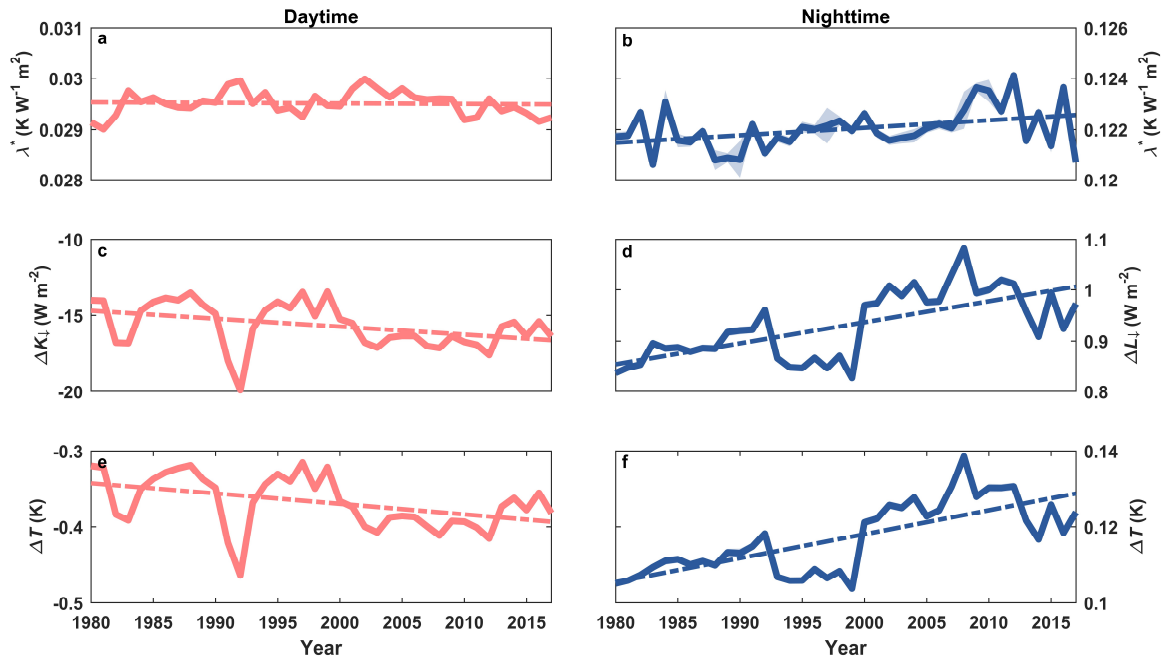


Figure S10. Long-term trends in **a**, daytime apparent surface climate sensitivity (λ^*), **b**, nighttime λ^* , **c**, daytime surface shortwave RE (ΔK_{\downarrow}), **d**, nighttime surface longwave RE (ΔL_{\downarrow}), **e**, daytime temperature perturbation, and **f**, nighttime temperature perturbation for the world's land surfaces. The dashed lines show the linear trends of the temporal variation. All long-term trends are statistically significant (p -value < 0.01).

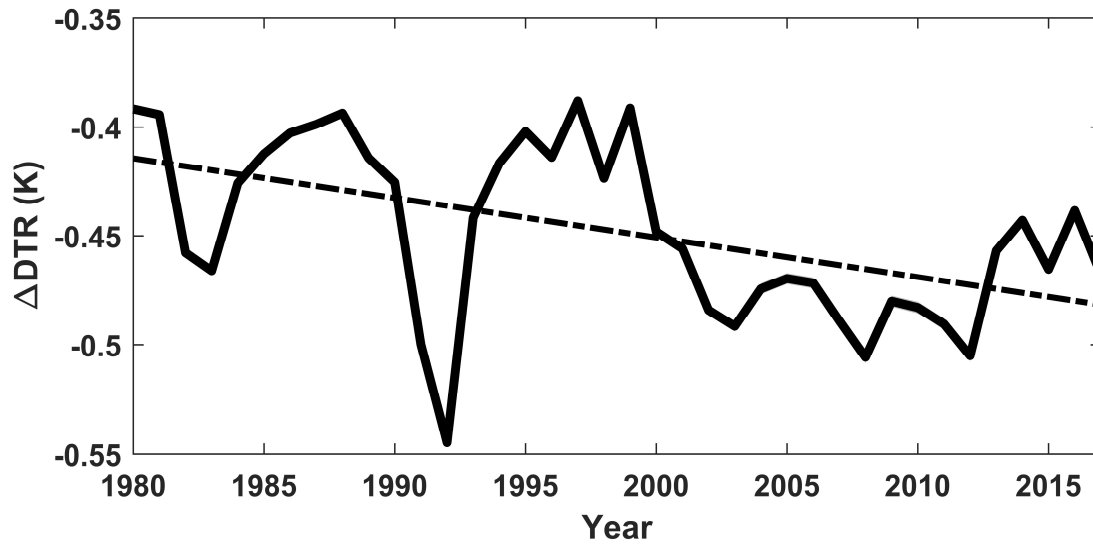


Figure S11. Long-term trend of diurnal temperature range perturbation for the world's land surfaces. The solid line shows the mean values while the shaded portion shows the standard error of the means. The standard errors are negligible. The dashed line shows the linear trend of the temporal variation. The long-term trend is statistically significant (p-value<0.01).

Supplementary Table S1. Summary of mean and standard deviation of the estimated variables for the world's land surfaces and each climate zone for 2008-2017. Here, f is the energy redistribution factor (unitless), λ_0 is the intrinsic climate sensitivity (in $\text{K W}^{-1} \text{m}^2$), λ^* is the effective local climate sensitivity (in $\text{K W}^{-1} \text{m}^2$), RE is the aerosol radiative effect (in W m^{-2}), ΔK_{\downarrow} is the aerosol RE in the shortwave band (in W m^{-2}), ΔL_{\downarrow} is the aerosol RE in the longwave band (in W m^{-2}), ΔT is the temperature perturbation (in K), and ΔDTR is the diurnal temperature range perturbation (in K).

Variable	Global	Equatorial	Arid	Temperate	Snow	Polar
Daytime (surface)						
f	6.98 ± 2.53	13.25 ± 7.71	3.47 ± 1.14	7.75 ± 2.99	6.73 ± 1.74	5.12 ± 1.00
λ_0	0.19 ± 0.02	0.16 ± 0.00	0.17 ± 0.01	0.18 ± 0.01	0.21 ± 0.01	0.22 ± 0.01
λ^*	0.029 ± 0.007	0.015 ± 0.007	0.041 ± 0.009	0.022 ± 0.006	0.029 ± 0.006	0.037 ± 0.006
ΔK_{\downarrow}	-16.40 ± 8.50	-18.31 ± 10.85	-24.94 ± 14.48	-17.40 ± 11.99	-9.62 ± 4.41	-6.44 ± 1.87
ΔL_{\downarrow}	1.01 ± 1.07	0.77 ± 0.82	2.25 ± 2.30	0.73 ± 0.75	0.26 ± 0.27	0.13 ± 0.14
ΔT (to ΔK_{\downarrow})	-0.39 ± 0.24	-0.27 ± 0.24	-0.75 ± 0.47	-0.33 ± 0.28	-0.20 ± 0.12	-0.17 ± 0.08
ΔT (to ΔL_{\downarrow})	0.039 ± 0.048	0.015 ± 0.021	0.110 ± 0.119	0.018 ± 0.023	0.007 ± 0.009	0.005 ± 0.007
Nighttime (surface)						
f	0.90 ± 0.32	0.73 ± 0.73	0.54 ± 0.27	0.62 ± 0.50	1.33 ± 0.62	1.02 ± 0.68
λ_0	0.21 ± 0.03	0.17 ± 0.00	0.20 ± 0.02	0.20 ± 0.01	0.24 ± 0.02	0.27 ± 0.02
λ^*	0.122 ± 0.025	0.115 ± 0.040	0.130 ± 0.023	0.132 ± 0.141	0.113 ± 0.034	0.146 ± 0.043
ΔL_{\downarrow}	0.99 ± 1.04	0.80 ± 0.84	2.26 ± 2.16	0.75 ± 0.75	0.25 ± 0.28	0.13 ± 0.15
ΔT (to ΔL_{\downarrow})	0.126 ± 0.131	0.105 ± 0.138	0.287 ± 0.269	0.107 ± 0.133	0.030 ± 0.042	0.018 ± 0.025
Annual (surface)						
f	4.21 ± 1.41	7.53 ± 4.42	2.13 ± 0.66	4.50 ± 1.74	4.29 ± 1.12	3.26 ± 0.76
λ^*	0.072 ± 0.013	0.061 ± 0.021	0.081 ± 0.012	0.072 ± 0.065	0.067 ± 0.018	0.087 ± 0.021
ΔT	-0.13 ± 0.06	-0.09 ± 0.08	-0.22 ± 0.10	-0.12 ± 0.10	-0.09 ± 0.05	-0.08 ± 0.03
ΔDTR	-0.47 ± 0.32	-0.36 ± 0.34	-0.93 ± 0.62	-0.42 ± 0.38	-0.22 ± 0.14	-0.18 ± 0.09
RE	-7.94 ± 3.64	-9.17 ± 5.34	-11.25 ± 5.80	-8.74 ± 5.89	-5.01 ± 2.18	-3.39 ± 0.94
Daytime (top of atmosphere)						
ΔK_{\downarrow}	-2.99 ± 1.40	-4.85 ± 2.65	-2.73 ± 3.68	-5.12 ± 3.32	-1.88 ± 1.51	-0.34 ± 0.84
ΔL_{\uparrow}	-0.29 ± 0.27	-0.23 ± 0.22	-0.67 ± 0.56	-0.19 ± 0.21	-0.09 ± 0.09	-0.05 ± 0.05
Nighttime (top of atmosphere)						
ΔL_{\uparrow}	-0.10 ± 0.07	-0.12 ± 0.09	-0.18 ± 0.14	-0.08 ± 0.07	-0.04 ± 0.04	-0.02 ± 0.02
Annual (top of atmosphere)						
Land RE	-1.43 ± 0.71	-2.46 ± 1.32	-1.04 ± 2.06	-2.65 ± 1.71	-0.96 ± 0.77	-0.15 ± 0.44
All RE	(-0.89 ± 0.27)					